Available online at www.sciencedirect.com
ScienceDirect
Ceramics International 35 (2009) 2053–2059
CERAMICS INTERNATIONAL
www.elsevier.com/locate/ceramint

Nanocrystalline ceramic coating on γ-TiAl by bipolar plasma electrolysis (effect of frequency, time and cathodic/anodic duty cycle)

M. Aliofkhazraei [a], S.A. Hassanzadeh-Tabrizi [a], A. Sabour Rouhaghdam [a,*], A. Heydarzadeh [b]

[a] Department of Materials Engineering, Faculty of Engineering, Tarbiat Modares University, P.O. Box: 14115-143, Tehran, Iran
[b] Biotechnology Group, Chemical Engineering Department, Tarbiat Modares University, P.O. Box: 14115-143, Tehran, Iran

Received 3 June 2008; received in revised form 19 September 2008; accepted 11 November 2008
Available online 3 December 2008

Abstract

The present work reports the usage of plasma electrolysis for nanocrystalline coating of γ-TiAl alloy by applying pulsed current in an organic electrolyte based on glycerol. Response Surface Methodology (RSM) was applied to optimize the operating conditions for small nanocrystallite sizes of coatings. The levels studied were the ratio of duty cycle of cathodic direction to duty cycle of anodic direction of 0.2–0.4, frequency of pulsed current range between 5 and 15 kHz, and treatment time of 10–30 min. The usage of high applied frequencies and low ratios of duty cycle of cathodic direction to duty cycle of anodic direction and also treatment time is more suitable for achieving lower sizes of complex nanocrystallites. The samples with high height to width ratio of distribution curves of nanocrystallites have simultaneously smaller average sizes of nanocrystallites and lower length to diameter ratio of nanocrystallites.

Keywords: A. Films; B. Electron microscopy; D. Borides; D. Carbides

1. Introduction

Attractive properties of titanium and titanium alloys lead to an ever increasing interest in using them in such areas as power generation, medical devices and automotive parts. Mainly their excellent specific strength and outstanding corrosion resistance have made them very important. However, their use is currently restricted to non-tribological applications, owing to their high friction and wear and a strong tendency to galling. Therefore, different surface engineering techniques have been developed in recent years to overcome the problems, e.g. a duplex process consisting of plasma nitriding or plasma carburizing with subsequent PACVD coating of TiC [1]. The establishment of hard films upon the surface is of great importance due to their superior mechanical, thermal and corrosion resistance properties [2].

Plasma electrolytic saturation (PES) technique was developed recently for surface modification of different metals in solution [3–6]. In the PES process, the work piece, which is served as a cathode in an electrolysis cell, is connected to a special power supply. Once a stable gas film is formed on the work piece by applied high voltage, electrical discharge, including electron and ion avalanche, occurs across the gas film. Then, the work piece is heated due to the generation of resistance heat in a short time, and the local temperature in the discharge area can reach a very high value, which can be above the austenite temperature. The hydrogen film around the work piece will break down after the power supply is shut off, and the surface of the work piece will be self-quenched by the cold electrolyte surrounding it, or the specimen can move out during the sparking and cool in the air.

Plasma electrolytic saturation for surface hardening of γ-TiAl by the means of complex carburizing and boriding is done in this investigation [7,8]. RSM was applied to optimize the operating conditions for the process. A 2^3 full factorial central composite design (CCD) was chosen to explain the combined effects of 3 parameters, i.e. ratio of duty cycle of cathodic direction to duty cycle of anodic direction, frequency of pulsed current and treatment time.

* Corresponding author. Tel.: +98 9126905626; fax: +98 2166960664.
E-mail address: sabour01@gmail.com (A. Sabour Rouhaghdam).

0272-8842/$34.00
doi:10.1016/j.ceramint.2008.11.005

2. Experimental procedure

2.1. Materials and methods

Disc samples made of the annealed γ-TiAl alloy (Ti–48Al–2Cr–2Nb (Al 33.5 wt.%, Cr 2.55 wt.%, Nb 2.67 wt.%, Ti balance)) with a diameter of 20 mm and thickness of 5 mm were grounded to different stages of metallographic polishing to obtain a near-mirror surface finish and then ultra-sonically cleaned in pure ethyl alcohol. Pulsed bipolar nanocrystalline plasma electrolytic carbo-boriding (PBNPEC/B) treatment was performed in a cooling vessel to maintain temperature of electrolyte constant at 40 °C. The treatment electrolyte was a mixed organic solution of glycerol and chemically pure dissolved borax and boric acid. Boric acid was added to provide a desirable electrical conductivity of electrolyte.

In this work, the workpieces were biased to pulsed current from a 20 kW power supply. An AISI 316 stainless steel cylinder of dimensions 15 cm dia × 22 cm formed the anode of the electrochemical system of coating process. An average current density of 0.5 A cm^{-2} was used during PBNPEC/B treatment. Morphologies and their quantitative analysis of the coatings were observed by the means of scanning electron microscopy (SEM). The studies were performed on a Philips XL-30 scanning electron microscope. In order to evaluate the hardness of the treated samples Vickers micro-hardness test was made with loads of 100 g having a maximum time of 15 s at the maximum load. Nine microhardness measurements were made on each sample and average result reported for higher accuracy. The wear resistance of the samples was studied using standard pin-on-disk wear test. They were subjected to a normal force of 50 N against the wheel rotating at a constant speed of 200 rpm. After 4000 m of sliding distance, the weight loss of samples was determined by a digital balance (Sartorious CP324S) with a resolution of 10^{-4} g.

To measure length to diameter ratio (L/D ratio) for nanocrystallites, 5 SEM nanostructures with same magnification were analyzed through commercial software for figure analysis called a4iDocu for each treated sample. Different measurements were interpolated to obtain average results. At least 40 measurements were done in each nanostructure for minimizing systematical errors. An example of obtained SEM figures can be seen in Fig. 1. The distribution of nanocrystals was plotted and they have shown a Gaussian-shape. It is well known that for achieving better properties of nanocrystalline layers, it is better to have this Gaussian-shape curve narrower, which shows distribution of sizes of nanocrystals around a particular amount. So the ratio of height to width (in the middle of curve) (H/W ratio) of these Gaussian-shape curves were measured and plotted for different treated samples. They have been studied in order to maximize this ratio.

2.2. Experimental design and optimization

For PBNPEC/B, the significant independent variables are ratio of duty cycle of cathodic direction to duty cycle of anodic direction, frequency of pulsed current and treatment time. In the present work, glycerol concentration was kept constant, since by preliminary trials (not reported here) it has been showed that this parameter will not affect process significantly [8].

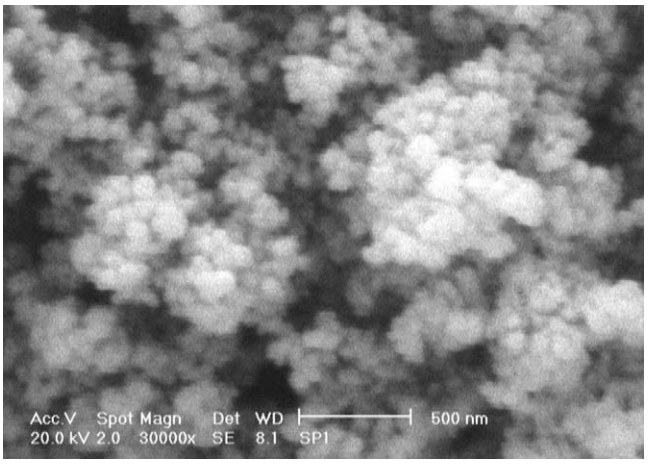

Fig. 1. An example of SEM nanostructure for a treated sample with average size of nanocrystallites around 85.6 nm.

For a scientific or engineering investigation concerned with a process or system response Y that depends on the input factors (also called input variables) $X1$, $X2$, $X3$, …, XK, the relationship between response and variables can be modeled by

$$Y = f(X1, X2, \ldots, XK) + \varepsilon \quad (1)$$

where ε is an error term that represents the sources of variability not captured by f. It is assumed that the ε over different runs is independent, and have mean zero.

In developing the regression equation, the test variables were coded according to the equation:

$$x_i = \frac{X_i - X_{cp}}{\Delta X_i} \quad (2)$$

where x_i is the independent variable coded value. X_i is the independent variable real value. X_{cp} is the independent variable real value at the centre point and ΔX_i is the step change of the real value of the variable 'i' corresponding to a variation of a unit for the dimensionless value of the variable 'i'.

The response variable (average size of nanocrystallites) was fitted by a second order model in order to correlate the response variables to the independent variables. The general equation of the second degree polynomial equation is

$$Y_i = \beta_0 + \sum \beta_i X_i + \sum \beta_{ij} X_i X_j + \sum \beta_{ii} X_i^2 + \varepsilon \quad (3)$$

where Y_i is the predicted response; X_i, X_j are input variables which influence the response variable Y; β_0 is the ith linear coefficient; β_{ii} is the quadratic coefficient and β_{ij} is the linear-by-linear interaction between X_i and X_j, where 'i' tends from 1 to 3.

A 2^3 full factorial CCD for three independent variables each at five levels with six star points and six replicates at the centre points was employed to fit a second order polynomial model which indicated 20 experiments to be required for this procedure. The 'Minitab 15' software was used for regression

and graphical analysis of the data obtained. The statistical analysis of the model was performed in the form of analysis of variance (ANOVA). This analysis includes the Fisher's F-test (overall model significance), its associated probability $P(F)$, correlation coefficient R, determination coefficient R^2 which measures the goodness of fit of regression model. It also includes the t-value for the estimated coefficients and associated probabilities, $P(t)$. For each variable, the quadratic models are represented as response surface plots.

3. Results and discussion

3.1. Optimization

The levels of the variables for minimum average sizes of nanocrystallites (ASN) were selected as the central points in the more elaborate second order experiment. In the RSM study, the three variables studied were ratio of duty cycle of cathodic direction to duty cycle of anodic direction ($X1$), frequency of pulsed current ($X2$) and treatment time ($X3$). The main goal of the second phase of the response surface was to obtain an accurate approximation to the response surface in a small region around the optimum and to identify optimum process conditions. The range and the levels of the variables investigated in the study are listed in Table 1. The central values (zero level) chosen for experimental design were 0.3 for the ratio of duty cycle of cathodic direction to duty cycle of anodic direction, 10 kHz for the frequency of pulsed current and 20 min for treatment time. In the quest for the optimum combination of the variables, experiments were performed according to the CCD experimental plan (Table 2). The experiment used a CCD which consists of three parts. The eight runs involving the '1' and '−1' coded values (Table 2) form a 2^3 design. Because they are on the corners of the 2^3 cube, they are called cube points or corner points. The six runs involving the '±1' and '0' coded values form three pairs of points along the three coordinate axes and are therefore called the axial points or star points. The two runs involving the '0' coded values are at the centre of the design region and are called the centre points. This design is a second order design, and it allows all the linear and quadratic components of the main effects and the linear-by-linear interactions to be estimated.

The results of the response surface model fitting in the form of ANOVA are shown in Table 3. The ANOVA of the quadratic regression model demonstrated the model to be significant with a low probability value ($P_{\text{model}} > F = 0.000$). The goodness of the fit of the model was checked by determination coefficient (R^2). In this case, the value of the determination coefficient, R^2 was 0.9996. The value of the adjusted determination coefficient is adj $R^2 = 0.9991$. Table 4 compares the RSM predicted and experimental average sizes of nanocrystallites.

The application of RSM yielded the following regression equation which is the empirical relationship between average sizes of nanocrystallites (Y_i) and the test variables in coded

Table 1
Experimental range and levels of the independent variables.

Variables	Range and levels		
	−1	0	+1
$X1$	0.2	0.3	0.4
$X2$	5	10	15
$X3$	10	20	30

Table 2
CCD plan in coded values and observed response (average sizes of nanocrystallites).

Experiment run no.	$X1$	$X2$	$X3$	Response
1	−1	−1	−1	55.2
2	1	−1	−1	85.4
3	−1	1	−1	32.5
4	1	1	−1	62.6
5	−1	−1	1	66.1
6	1	−1	1	95.1
7	−1	1	1	42.4
8	1	1	1	72.6
9	0	0	0	58.2
10	0	0	0	58.5
11	−1	0	0	42.9
12	1	0	0	72.6
13	0	0	−1	52.6
14	0	0	1	63.4
15	0	−1	0	75.9
16	0	1	0	51.7

Table 3
ANOVA for the quadratic model.

Source	SS	DF	MS	F-value	$P > F$
Model	3964.22	9	440.47	1812.70	0.000
Residual (error)	1.46	6	0.24		
Pure error	0.05	1	0.05		
Total	3965.67	15			

SS: sum of squares; DF: degrees of freedom; MS: mean square.

Table 4
The measured and predicted response values, together with the values for the residuals and the standard errors.

Experiment run no.	Measured	Predicted	Residuals	Standard error
1	55.2	55.401	−0.201	−0.90
2	85.4	85.241	0.159	0.71
3	32.5	32.121	0.379	1.70
4	62.6	62.511	0.089	0.40
5	66.1	66.111	−0.011	−0.05
6	95.1	95.401	−0.301	−1.35
7	42.4	42.481	−0.081	−0.36
8	72.6	72.321	0.279	1.25
9	58.2	58.036	0.164	0.38
10	58.5	58.036	0.464	1.07
11	42.9	42.987	−0.087	−0.26
12	72.6	72.827	−0.227	−0.67
13	52.6	53.027	−0.427	−1.26
14	63.4	63.287	0.113	0.34
15	75.9	75.547	0.353	1.05
16	51.7	52.367	−0.667	−1.98

Table 5
The least-squares fit and coefficient estimates (significance of regression coefficients).

Model term	Coefficient	Standard error	*t* ratio	*P*-value
Constant	58.0362	0.2334	248.684	0.000
*X*1	14.9200	0.1559	95.714	0.000
*X*2	−11.5900	0.1559	−74.351	0.000
*X*3	5.1300	0.1559	32.910	0.000
*X*1 × *X*1	−0.1293	0.3036	−0.426	0.685
*X*2 × *X*2	5.9207	0.3036	19.502	0.000
*X*3 × *X*3	0.1207	0.3036	0.398	0.705
*X*1 × *X*2	0.1375	0.1743	0.789	0.460
*X*1 × *X*3	−0.1375	0.1743	−0.789	0.460
*X*2 × *X*3	−0.0875	0.1743	−0.502	0.634

units.

$$Y_i = 58.04 + 14.92X1 - 11.59X2 + 5.13X3 - 0.13(X1 \times X1) + 5.92(X2 \times X2) + 0.121(X3 \times X3) + 0.14(X1 \times X2) - 0.14(X1 \times X3) - 0.088(X2 \times X3) \quad (4)$$

where Y_i is the predicted response. *X*1, *X*2 and *X*3 are the coded values of the test variables viz. ratio of duty cycle of cathodic direction to duty cycle of anodic direction, frequency of pulsed current and treatment time, respectively.

The significance of each coefficient determined by *t*-test and *P*-values are listed in Table 5. Larger magnitudes of the *t*-value and smaller amounts of the *P*-value will lead to the more significant of the corresponding coefficient. Values of $P < 0.0500$ indicate model terms to be significant. The response surface plots are generally the graphical representations of the regression equation and are presented in Figs. 2–4 from which the values of average sizes of nanocrystallites for different levels of the variables can be predicted. Each response plot represents an infinite number of combinations of two test variables with the other maintained at its respective zero level.

From the solutions predicted by the model, the experimental conditions set at ratio of duty cycle of cathodic direction to duty cycle of anodic direction at 0.2, frequency of pulsed current at 14.9 kHz and treatment time at 10 min and it could give average sizes of nanocrystallites at 32 nm.

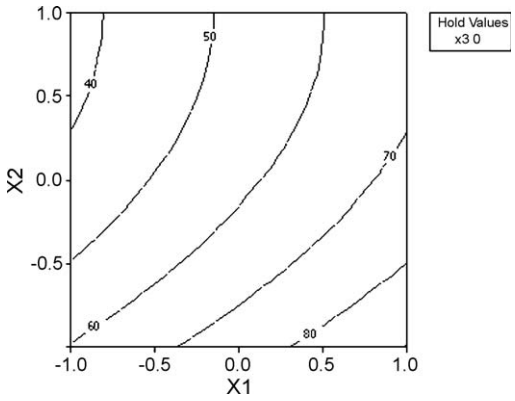

Fig. 2. Contour plot between *X*1 and *X*2 when *X*3 is hold at zero level.

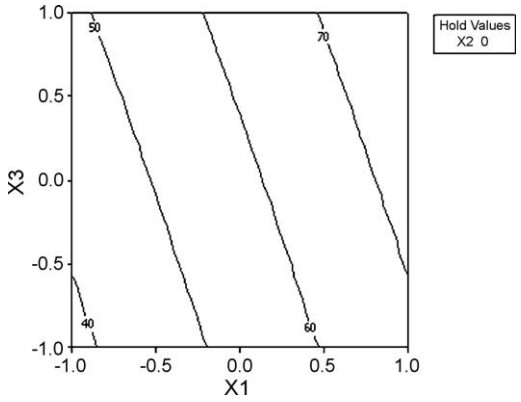

Fig. 3. Contour plot between *X*1 and *X*3 when *X*2 is hold at zero level.

3.2. Average size of nanocrystallites

Fig. 5 shows the average sizes of nanocrystallites of different samples found through the process. The minimum average size of nanocrystallites was found to be 32.5 nm for sample 3. From the above results, it can easily be said that lower average sizes of nanocrystallites have been obtained with higher applied frequencies and lower ratios of duty cycle of cathodic direction to duty cycle of anodic direction and treatment times.

3.3. L/D ratio

Fig. 6 shows the L/D ratio of nanocrystallites for different samples found through the process. The minimum L/D ratio of nanocrystals was found to be 1.3. Smaller L/D ratios show that nanocrystals have shapes like spheres. As it can be seen the samples that have smaller L/D ratio of nanocrystals also have smaller average sizes of nanocrystallites.

3.4. H/W ratio

Fig. 7 shows the height to width (H/W) ratio of distribution curves for nanocrystallites of different samples. The maximum H/W ratio was found to be 11.5. Comparing with other obtained results, it can be seen that the samples with high H/W ratio have

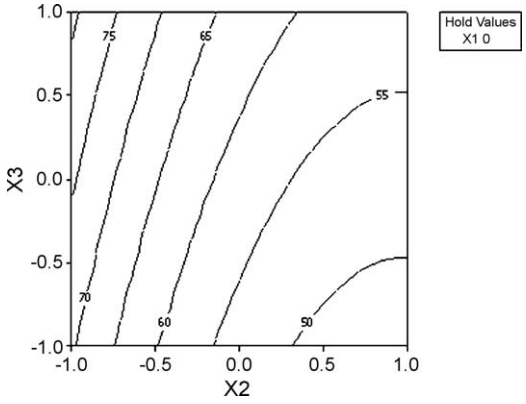

Fig. 4. Contour plot between *X*2 and *X*3 when *X*1 is hold at zero level.

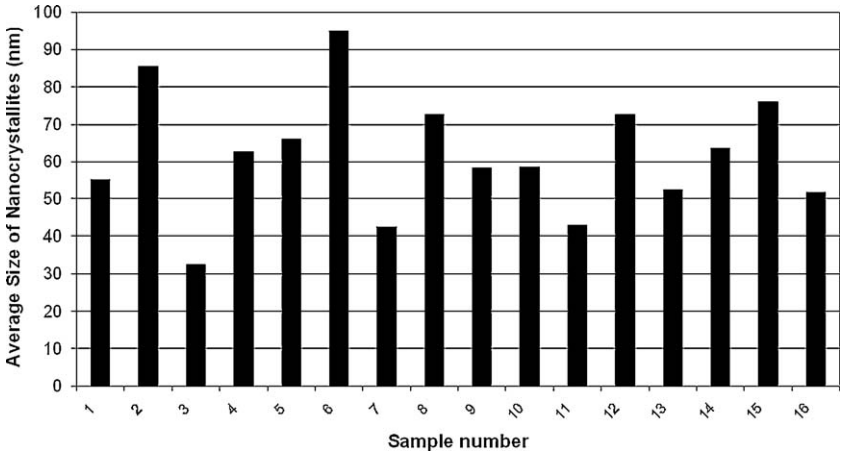

Fig. 5. Average size of nanocrystallites for different treated samples.

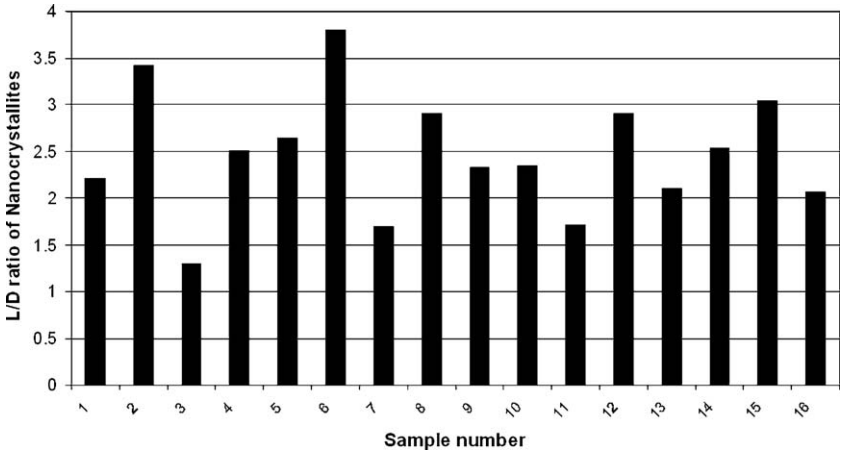

Fig. 6. L/D ratio of nanocrystallites for different treated samples.

smaller average sizes of nanocrystallites and lower L/D ratios. High distribution of nanocrystals around a specific average value will lead to better corrosion and wear resistances. Samples with lower amounts of this average value show better wear and corrosion characteristics.

3.5. Similar trend of changes for different properties of coated samples

Fig. 8 shows the layers thicknesses as well as micro-hardnesses and mass loss due to wear tests of coated samples.

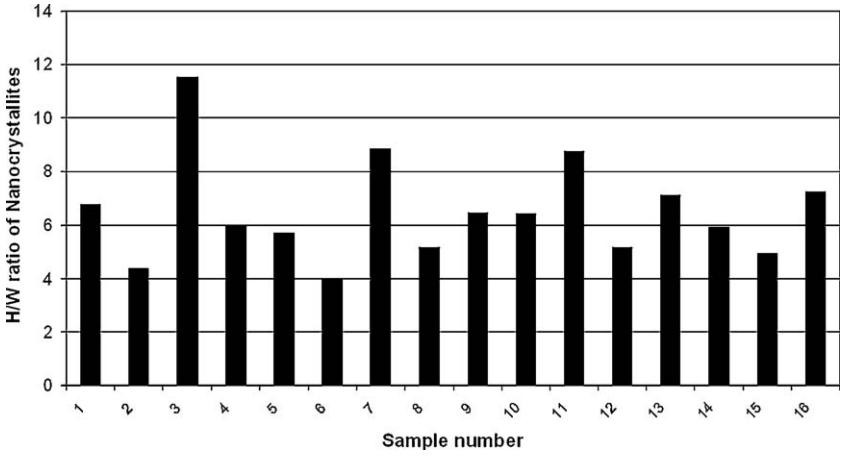

Fig. 7. H/W ratio of nanocrystallites for different treated samples.

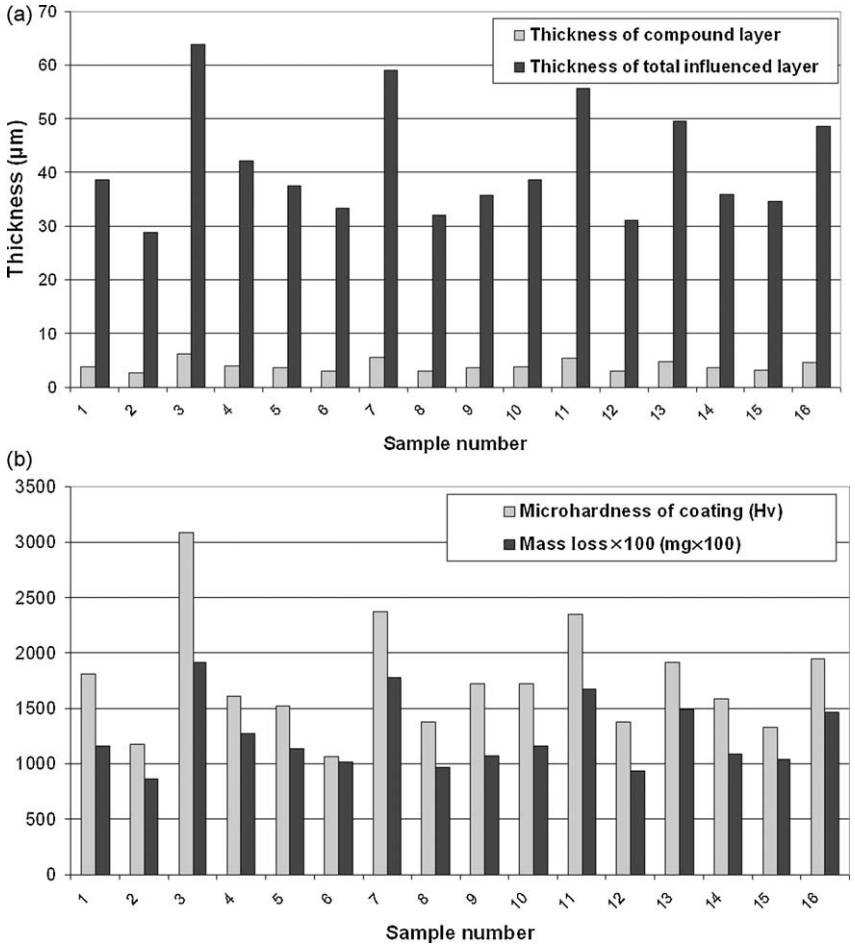

Fig. 8. (a) Thicknesses of compound layer and total influenced layer of different treated samples and (b) micro-hardnesses and mass losses (100×) of different treated samples.

Very strong relation among these properties of coatings will show their dependence to nanostructure of hard layer. In fact, adjusting the effective parameters of plasma electrolysis for decreasing the average size of nanocrystallites will lead to better over all properties of treated samples.

4. Conclusion

RSM proved to be fairly accurate in predictive modeling and optimization of conditions for minimizing the average sizes of nanocrystallites obtained in pulsed bipolar nanocrystalline plasma electrolytic carbo-boriding (PBNPEC/B), and that the average sizes of nanocrystallites to be reasonably approximated by quadratic non-linearity. In this process, the samples with high height to width ratio of distribution curves of nanocrystallites have smaller average sizes of nanocrystallites and lower length to diameter ratio of nanocrystallites. Also different treated samples show similar trends of changes in their properties, related to the nanostructure of compound layer.

Acknowledgments

The authors wish to express their thanks to Dr. James Curran (Cambridge University) for his useful guides during the course of investigation about different aspects of plasma electrolysis. This project is funded by Arvandan Oil and Gas Production Company (TMU 85-09-66) and Iranian nanotechnology initiative.

References

[1] P. Kaestner, J. Olfe, J.W. He, K.T. Rie, Improvement in the load-bearing capacity and adhesion of TiC coatings on TiAl6V4 by duplex treatment, Surface and Coatings Technology 142–144 (2001) 928.
[2] N. Matuda, S. Baba, A. Kinbara, Mechanical properties of boron films, Thin Solid Films 89 (1982) 139.
[3] A.L. Yerokhin, X. Nie, A. Leyland, A. Matthews, S.J. Dowey, Plasma electrolysis for surface engineering, Surface and Coatings Technology 2–3 (1999) 73.
[4] M. Aliofkhazraei, P. Taheri, A.R. Sabour, Ch. Dehghanian, Study of nanocrystalline plasma electrolytic carbonitriding for CP-Ti, Materials Science 43 (6) (2007) 791.
[5] M. Aliofkhazraei, A. Sabour Rouhaghdam, M. Sabouri, Effect of frequency and duty cycle on corrosion behavior of pulsed nanocrystalline plasma electrolytic carbonitrided CP-Ti, Journal of Materials Science 43 (2008) 1624.
[6] M. Aliofkhazraee, A. Sabour Rouhaghdam, T. Shahrabi, Pulsed nanocrystalline plasma electrolytic carburising for corrosion protection of a γ-TiAl alloy: Part 1. Effect of frequency and duty cycle, Journal of Alloys and Compounds 460 (2008) 614.

[7] P. Taheri, Ch. Dehghanian, M. Aliofkhazraei, A.R. Sabour, Nanocrystalline structure produced by complex surface treatments: plasma electrolytic nitrocarburizing, boronitriding, borocarburizing, and borocarbonitriding, Plasma Processes and Polymers 4 (2007) S721.

[8] M. Aliofkhazraee, A. Sabour Rouhaghdam, Pulsed nanocrystalline plasma electrolytic carburising for corrosion protection of a γ-TiAl alloy: Part 2. Constant frequency and duty cycle, Journal of Alloys and Compounds 462 (2008) 421.